

## Numerical characterization of real railway overhead cables

Cristina Sanchez-Rebollo<sup>1</sup>, Enrique Velez<sup>2</sup> and Jesus R. Jimenez-Octavio<sup>\*2</sup>

<sup>1</sup>*Institute for Research in Technology, Universidad Pontificia Comillas, c/ Santa Cruz de Marcenado 26, 28015 Madrid, Spain*

<sup>2</sup>*Department of Mechanical Engineering, Universidad Pontificia Comillas, c/ Alberto Aguilera 23, 28015 Madrid, Spain*

*(Received October 10, 2014, Revised May 21, 2015, Accepted May 25, 2015)*

**Abstract.** This paper presents a numerical characterization of real railway overhead cables based on computational fluid dynamics (CFD). Complete analysis of the aerodynamic coefficients of this type of cross section yields a more accurate modelling of pressure loads acting on moving cables than provided by current approaches used in design. Thus, the characterization of certain selected commercial cables is carried out in this work for different wind speeds and angles of attack. The aerodynamic lift and drag coefficients are herein determined for two different types of grooved cables, which establish a relevant data set for the railway industry. Finally, the influence of this characterization on the fluid-structure interaction (FSI) is proved, the static behavior of a catenary system is studied by means of the finite element method (FEM) in order to analyze the effect of different wind angles of attack on the stiffness distribution.

**Keywords:** aerodynamic characteristics; overhead catenary line; CFD simulation; cable; lift force

---

### 1. Introduction

Railway systems are designed to withstand diverse loads and service cases during their service lives. However the current trends in design for railway lines are increasingly sensitive to wind effects when high speed trains run on them. Lateral wind gusts may induce structural loads, not only on the rolling stock, but also on the overhead catenary lines and the rest of the infrastructure. Nowadays wind loads acting on a vehicle are decreased by means of protection devices, such as fences or parapets, whose design and effectiveness under cross-winds has been analyzed experimentally by Kwon *et al.* (2001) and Barcala and Meseguer (2007) and, more recently, by Zheng (2009). These results converge that the presence of high enough parapets may result into important reductions of the wind load coefficients. Nonetheless, there is a lack of research towards the effects of cross-wind on the overhead catenary lines and its aerodynamic characterization.

Cross-wind loads may have far from negligible impacts on the rail network operation since strong gusts can affect the security of the service, even causing derailments and overturns. Suzuki *et al.* (2003) states that at least 29 accidents have happened due to wind in Japan since railway transport was installed in 1872, e.g., one of the most recent occurred in 1992 and is described in Imai *et al.* (2002). In addition, without reaching such extreme consequences as the previously

---

\*Corresponding author, Professor, E-mail: [joctavio@comillas.edu](mailto:joctavio@comillas.edu)

mentioned ones, wind forces on the wires of the catenary produce a *blow-off* directly proportional to the incident loads together with large vibration amplitudes on the overhead contact cables. These static and dynamic phenomena can produce delays and even cancellations of services, as is described in Johnson (1996) and Stickland and Scanlon (2001). Some other well-known incidents related to lateral wind loads are, for instance, the buckling of the steady arms, as depicted in the Finite Element Model showed in Fig. 1, the loss of contact of the pantograph running off the contact wire, and even the dewirement of the collector head. Naturally, maximum allowable deflections of the overhead catenary lines are limited by the operating range of the strips of the pantograph. Thus, the design of the cables structure, pantographs and even the rolling stock gauges, strongly depends on wind loads, CENELEC (2009a).

Generally speaking, the catenary-pantograph system is aimed at ensuring electric power supply reliably and continuously specially when high speed lines are considered. Thus, apart from the aerodynamic effects due to incident wind on the vehicles and pantograph, whose time-varying response may have an effect on the contact quality, what appears is both the abovementioned lateral deviations of the catenary and flow induced oscillations on the contact wire. These dynamic instabilities may turn up as a consequence of the mechanical properties of the cable structure in combination with the aerodynamic forces induced by the incident flow. There are certain phenomena which lead to such oscillations, grouped together as flow-induced vibrations, see Paidoussis (2011). Thus, such triggering mechanisms as aeolian vibrations due to the vortex shedding excitation, wake-induced flutter and mainly galloping instabilities, see Meseguer *et al.* (2001), are crucial to analyze railway overhead stability. The galloping of the overhead catenary cables, which nowadays is the major impediment to increasing trains speed, is defined by the aerodynamic coefficients and how they change when varying the angle of attack. Due to the more exacting quality requirements, the last European guidelines, see CENELEC (2002b), this has led to a more thorough focus on some dynamic phenomena and, therefore, the wind effects may become a limiting factor of the maximum allowable speed. In fact, the lateral deviation of the contact wire under the action of a cross-wind all govern the interoperability of the rail network, see European Railway Agency (2009).

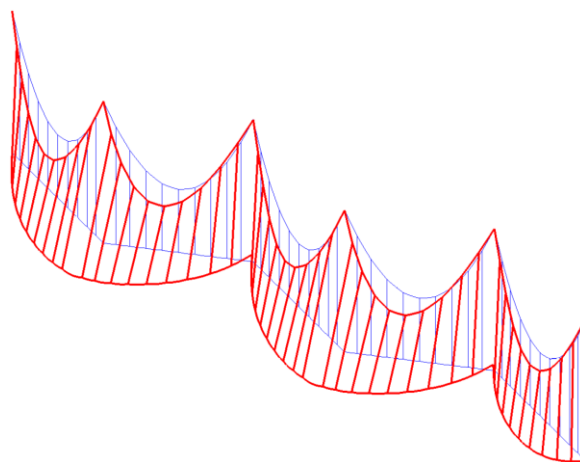


Fig. 1 Blow-off FEM simulation

The last phenomenon is the one related to the den Hartog criterion, which establishes that the instability will take place when

$$\frac{\partial C_L}{\partial \alpha} + C_D < 0 \quad (1)$$

where  $\alpha$  is the angle of attack of the wind and  $C_D$  and  $C_L$  are drag and lift coefficients, respectively.

Therefore, this aeroelastic instability occurs when there are geometrical asymmetries that produce a pressure gradient (lift force) that depends on the attack angle. As a circular cable does not cause this phenomenon, this instability is usually analyzed in the case of a circular cable with a drop, for instance Stickland and Scanlon (2001), but in the case of railway catenary cable, its own section leads to this instability.

The aim of this paper is to characterize the aerodynamic coefficients  $C_D$  and  $C_L$  of real railway overhead cables, which allow for the evaluation of the aeroelastic instability phenomenon in the context of railway systems. Therefore, static simulations of the contact wire during a gale have been computed and are presented in Section 3 in order to obtain the aerodynamic coefficients in different situations. Simulations have been made with 2 types of grooves, 3 different speeds of the wind and a wide range of attacking angles from  $-30^\circ$  to  $60^\circ$ . A brief mesh convergence study has been performed in order to guarantee the optimal compromise between the accuracy of the model and its computational cost. Finally, the influence of this study on the static catenary design is illustrated in Section 4 before the final concluding remarks of Section 5.

## 2. State of the art

Aerodynamic forces on cable structures have been studied by many authors from myriad points of view and purpose. Regarding the aim of the work herein accomplished, Yamaguchi (1990) presents an approach for the aerodynamic coefficients calculation by simulating an inclined cable with a moving rivulet in a wind-rain tunnel. Nevertheless, Gu *et al.* (2000) obtain those coefficients for a horizontal cylinder in a wind tunnel with fixed rivulet. More recently, Holmes (2015) presents the drag characterization for laminar flow incident on a cylinder, whose approximate value for the drag coefficient,  $C_D$ , is 1.2 when Reynolds numbers lower than  $2 \cdot 10^5$  are assumed. However, if the Reynolds number increases from here,  $C_D$  comes down to 0.4 at  $Re \approx 5 \cdot 10^5$ , but increasing  $Re$  again  $C_D$  climbs up to about 0.7 when  $Re \approx 10^7$ .

Classic fluid dynamics states that the downstream flow of a cylinder located perpendicularly to an incident uniform current has an alternating and periodic vortex shedding known as von Karman vortex street. Its matching with the natural frequencies of the structure could even cause a resonance phenomenon, e.g., the recently registered huge oscillations during the construction of an arch in the Spanish arch bridge of *La Plata* highway, see Alonso *et al.* (2007a). Nonetheless, cross galloping is another source of dynamic instability, much closer to slender structures and particularly to cable systems, which may appear in those asymmetric cross sections such as overhead catenary wires. Certain geometric and wake conditions may lead to large amplitude oscillations in the transverse direction of the incident wind, from 1 to 10 times bigger than the cross section of the structure, at much lower frequencies than the vortex shedding do, see for instance Alonso *et al.* (2005), Alonso and Meseguer (2006) and Alonso (2007b).

A different type of galloping may appear when an obstacle is placed in another's wake. Due to

the wake vortex generated by the first obstacle, the second one receives an incident current with time-varying intensity and direction, thus it tends to oscillate as Bricka and Laneville (1999), Hover and Triantafyllou (2001) and Flamand and Leclair (2005) state. Overhead transport systems may show this type of gallop since these electric lines run grouped in sets, consisting of several parallel wires, see Zdero and Turan (1995), and windbreak parapets also generate incident wakes as discussed by Stickland *et al.* (2000) for railway systems. This galloping only occurs when the natural frequencies of the downstream obstacle are lower than the vortex shedding frequency, as is pointed out in Meseguer *et al.* (2001), therefore the usual ways to prevent it, apart from decreasing the distance between spacers, is either to increase the mechanical tension of the cables and their natural frequencies, see Gurung *et al.* (2003), or to add mechanical damping as proposed by Stickland and Scanlon (2001).

Wind effects on the catenary-pantograph dynamic interaction are specifically referenced just in a very few references. For the droppers, steady arms and messenger wire, which are assumed as circular cross-section wires, the coefficients of drag and lift are taken one and zero respectively following the European Standard EN 50119, see CENELEC (2009b). Nevertheless, the contact wire presents grooves in order for it to be clamped and joined to the droppers that modify the symmetry of the cross section, so the variation of drag coefficient and a difference of pressures lead to the consideration of lift force. Recently, Liu *et al.* (2014) purposely analyses railway catenary wires under wind load by means of the Newton method; using wind tunnel tests, it considers different angles of attack, and so the dependence on aerodynamic coefficients of this variable is given for different wind speeds. However, these values do not refer any particular catenary or contact wire, and do not state whether the coefficient values are for the whole system or for a particular wire. Besides, in the previous works Stickland and Scanlon (2001) and Stickland *et al.* (2003) experimentally determined the aerodynamic coefficients of typical cross-sections of contact wires, although not commercial ones, prior to using the den Hartog criterion to see whether it is damp or not. Apart from that Bocciolone *et al.* (2006) presents the aerodynamic effects that the rolling stock generates on the pantograph, as well as the incident wind turbulence on the catenary-pantograph dynamic interaction. Finally Collina *et al.* (2007) accomplishes the active control of a pantograph, whose energy source is the incident wind and the control strategy is based on the catenary-pantograph dynamic simulation.

### 3. CFD Cable characterization

Considering the cable structure motion in the wind flow, an accurate evaluation of wind pressure on each type of overhead conductor is absolutely necessary for further FSI analysis. Thus, the main goal of this paper is the aerodynamic characterization of the cross section of real overhead catenary cables. Regarding some widespread commercial cross sections for high speed trains, their main geometry descriptors are gathered in Table 1.

Assuming AC-type are the most usual cables, in order to avoid being too tedious, only AC-80 and AC-150 are studied in this work. Fig. 2 explains the dimensional parameters and shows that all the dimensions of both selected cables correspond to the largest and the smallest of the whole set. Namely, AC-150 grooved cable has a similar shape to AC-120, AC-107 and AC-100, but AC-80 differs from those in its uppermost part.

Table 1 Geometric dimensions of commercial overhead catenary cables

Designation	Section [mm <sup>2</sup> ]	a [mm]	b [mm]	c [mm]	d [mm]	r [mm]
AC-80	80	5.6	8.0	3.8	10.6	0.4
AC-100	100	5.6	8.6	4.0	12.0	0.4
AC-107	107	5.6	8.6	4.0	12.3	0.4
AC-120	120	5.6	8.6	4.0	13.2	0.4
AC-150	150	5.6	8.6	4.0	14.8	0.4

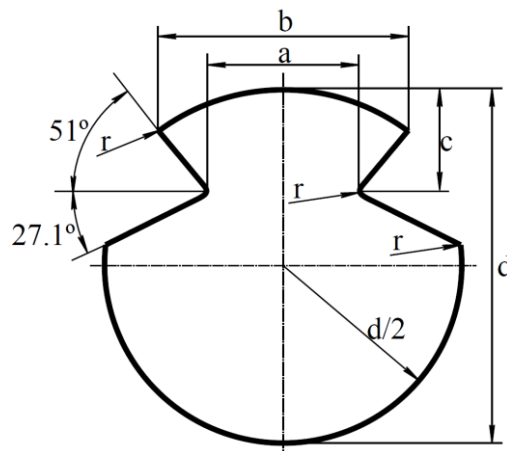


Fig. 2 Sketch of an overhead catenary line cross section

Holmes (2015) states that the type of event which produces the highest wind speed in the middle-latitudes, from about  $40^\circ$  to  $60^\circ$ , is a large depression. Thus, the conditions modelled in this work are aimed at simulating large depression states. Regardless of the Beaufort scale highest wind speed, considering the average speed during 10 minutes, it just reaches 32.5 m/s, in Kiessling *et al.* (2001) it is assured that wind speed design criteria ranges from 26 m/s up to 38.3 m/s in France and Germany. In fact, if the wind speed reaches 42 m/s, it could be considered a hurricane. Furthermore, the absolute maximum value of 42.2 m/s reported by Holmes as the data of annual wind speed maximum recorded in East Sale, Australia, from 1952 until 1998, is likely to be produced by a downburst. Thus, the simulations developed in this paper take speeds of 20, 30 and 40 m/s and sweep angles of attack from  $-30^\circ$  to  $60^\circ$ .

For statistical turbulence models, there exist numerous common two-equation and Reynolds-stress models. Nonetheless, the widely tested Shear Stress Transport (SST) turbulence model offers significant advantages for non-equilibrium turbulent boundary layer flows and heat transfer predictions. Recognized CFD simulation programs state that the SST model is as economical as the widely used  $k-\epsilon$  model, but it offers much higher fidelity, especially for separated flows, providing excellent answers on a wide range of flows and near-wall mesh conditions. Namely, SST model is a combination of the  $k-\epsilon$  in the free stream and the  $k-\omega$  models near the walls. It does not use wall functions and tends to be most accurate when solving the flow

near the wall.

Regarding certain parameters required for this purpose, the turbulence intensity is commonly fixed at 20% for gales from large depressions and the roughness length in open terrain ranges from 0.01 to 0.05 meters. Usually the calculation of the turbulence intensity assumes, according to Holmes (2015), a roughness length of 0.04 and a gale from a large depression. Finally, the turbulent viscosity rate is also estimated among the usual range of values, from 1 to 10.

In order to develop an accurate CFD model, taking mesh, boundary and solving conditions into consideration is essential. Some parameters related to those have to be obtained from different sources, but others are estimated by simulating a circular cylinder within laminar flow. The boundary layer theory states that it ends when the fluid speed moves at velocities that differ in less than a 1% to the free flow velocity, so consequently the dimensions of the surface are estimated. To conclude the modelling, the discretization of the domain is made up of quadrilateral elements to avoid the truncate error that appears when using triangles. The number of elements and refinement of the mesh also has to be estimated, taking into account that its design is usually revealed as a crucial part due to too fine meshes potentially cause excessive computational time, while coarser ones could converge into inaccurate solutions.

### 3.1 Numerical results

The purpose of this section is to scan the aerodynamic forces for each type of grooved cable and angle of attack of the wind speed, considering positive angle of attack in the direction shown in Fig. 3.

According to the knowledge acquired for circular-section cables (which have not been analyzed thoroughly herein to avoid being too long-winded), bi-dimensional squared shaped surfaces of 200×200 mm and 300×300 mm have been performed for cables AC-80 and AC-150 respectively. Only these two commercial cables are analysed according to the reasons set forth at the beginning of Section 3.

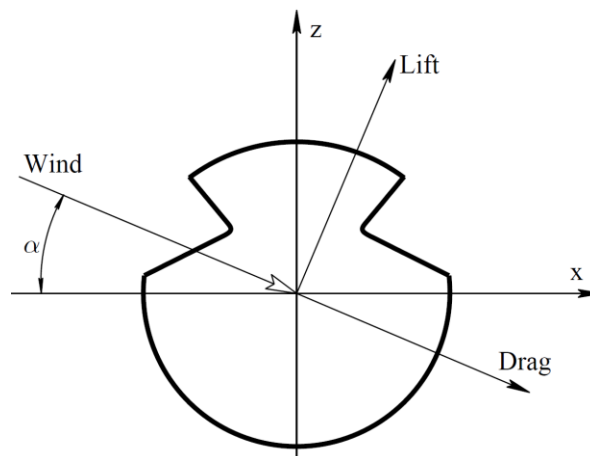


Fig. 3 Coordinate system for Lift-Drag forces

The Shear Stress Transport (SST) turbulence model has been applied with 20 percent turbulence intensity and a rate of turbulent viscosity of 10. The value of 20 percent involves very turbulent flow, but is suitable for the purpose of this work. From the purely numerical point of view, second order integration schemes have been selected and usual maximum number of iterations and order of magnitude for residuals have been fixed. Finally, there have been applied inlet-velocity condition for three edges and pressure-outlet condition for the other edge of the boundary.

Assuming these parameters and boundary conditions, a brief finite element mesh convergence study has been performed in order to guarantee the optimal compromise between the accuracy of the model and its computational cost. The study summarized in Table 2 for AC-80 under a wind load of 40 m/s with an angle of attack of 60° analyses four different meshes. Regarding the convergence of drag and lift coefficients dependent on the mesh quality (density of nodes, skewness and orthogonality), this study allow us to conclude that the optimal number of elements for the mesh around the grooved cables is obtained with Mesh #2, i.e.,  $45 \cdot 10^3$  elements for AC-80 and  $70 \cdot 10^3$  for AC-150.

Thus, taking the previously mentioned parameters and finite element mesh, the simulations AC-80 and AC-150 have been carried out at wind speeds of 20, 30 and 40 m/s and angles of attack of -30°, 0°, 30° and 60°. All of them have evidenced a good convergence and parameter  $y^+$  much lower than 1.

Firstly, from a qualitative point of view, Figs. 4(a) and 4(b) shows a noticeable depression under the cable when the angle of attack is 0°, although the higher this angle becomes, the more negligible the depression is. In spite of this analysis has been carried out at different wind velocities and angles of attack, the figure only shows the comparison between two angles of attack, 0° and 60° respectively, on an AC-80 type inside a wind flow of 40 m/s. This result has been observed and the same conclusion can be inferred, indeed, for both contact wires at all wind velocities tested.

Holmes (2015) claims that, for a smooth cylinder in an air flow, the aerodynamic drag coefficient is 1.2 for small Reynolds number, goes down to 0.4 by increasing Reynolds Number and goes up to 0.7 again. Nevertheless, when grooved cables are considered, the coefficient  $C_D$  depicted in Figs. 5(a)-5(c) and 6(a)-6(c) takes values from 0.65 to 0.9, reaching the highest value at 20 m/s and the smallest one at 40 m/s.

Regarding the general tendencies of the obtained results, it is clear that both drag and lift coefficients undergo major variations with the angle of attack, but otherwise they are quite stable to wind speed. Namely, the lift coefficient experiences a substantial increase from around 30°, independently to speed and cable.

Table 2 Mesh convergence study for AC-80 under wind load of 40 m/s at 60°

Mesh	$C_D$	$C_L$	Elements	Skewness	Orth. Quality
#1	0.6510	-0.0064	3378	0.604	0.382
#2	0.6719	0.6305	44968	0.551	0.532
#3	0.7126	0.5953	486736	0.520	0.645
#4	0.6944	0.6120	504358	0.502	0.638

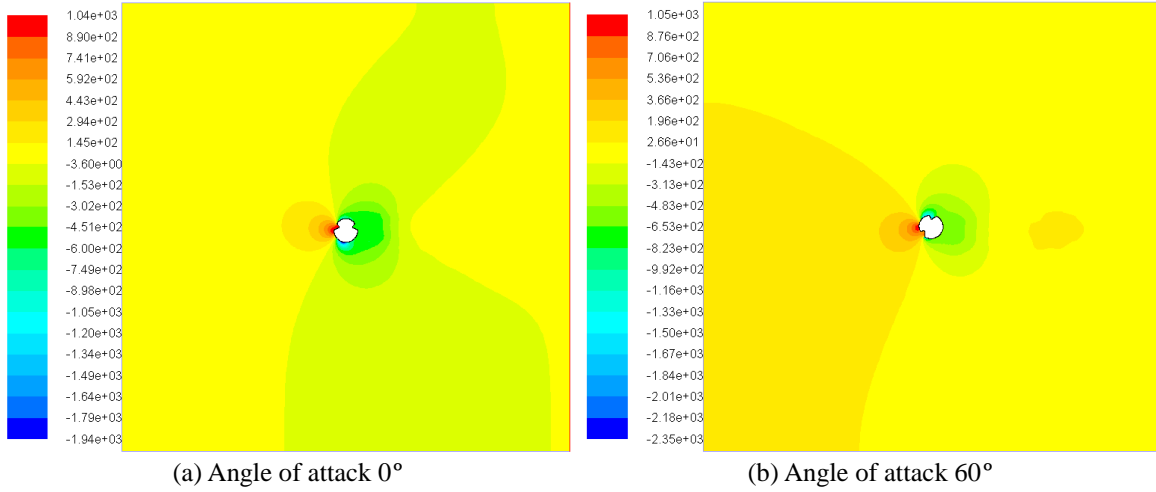


Fig. 4 Pressure distribution [Pa] around an AC-80 cable subjected to 40 m/s wind flow

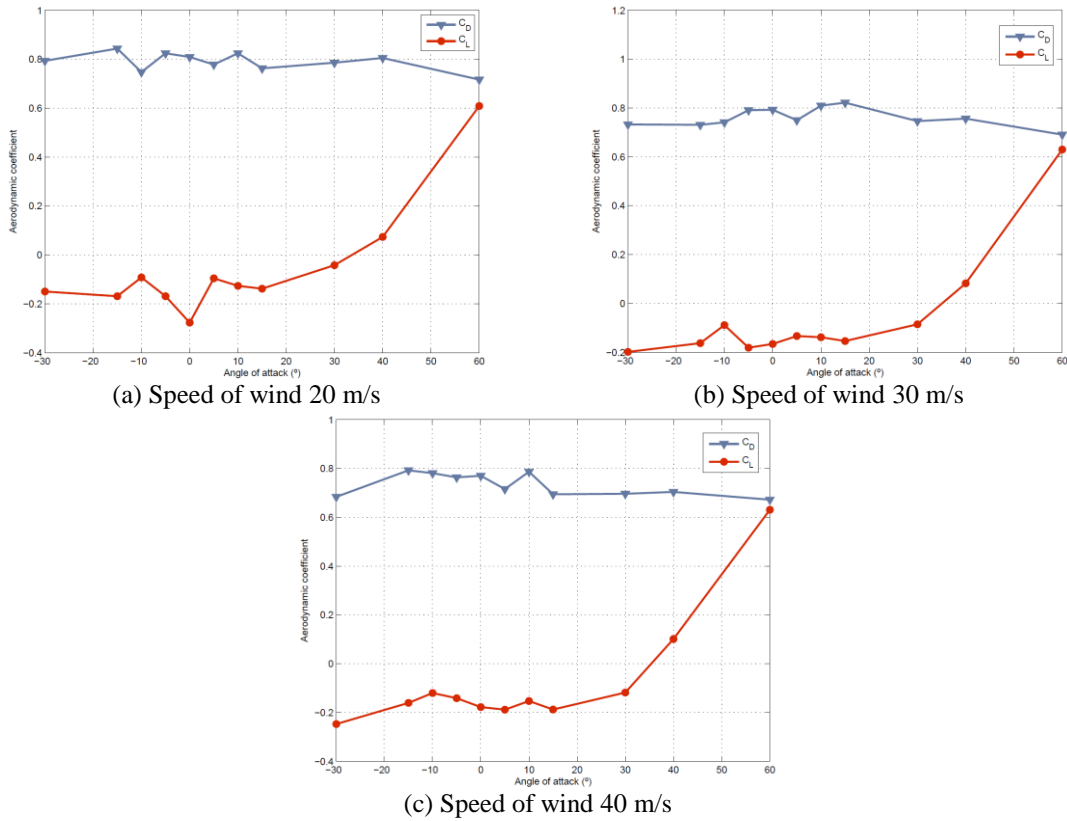


Fig. 5 Aerodynamic coefficients for AC-80 catenary cable

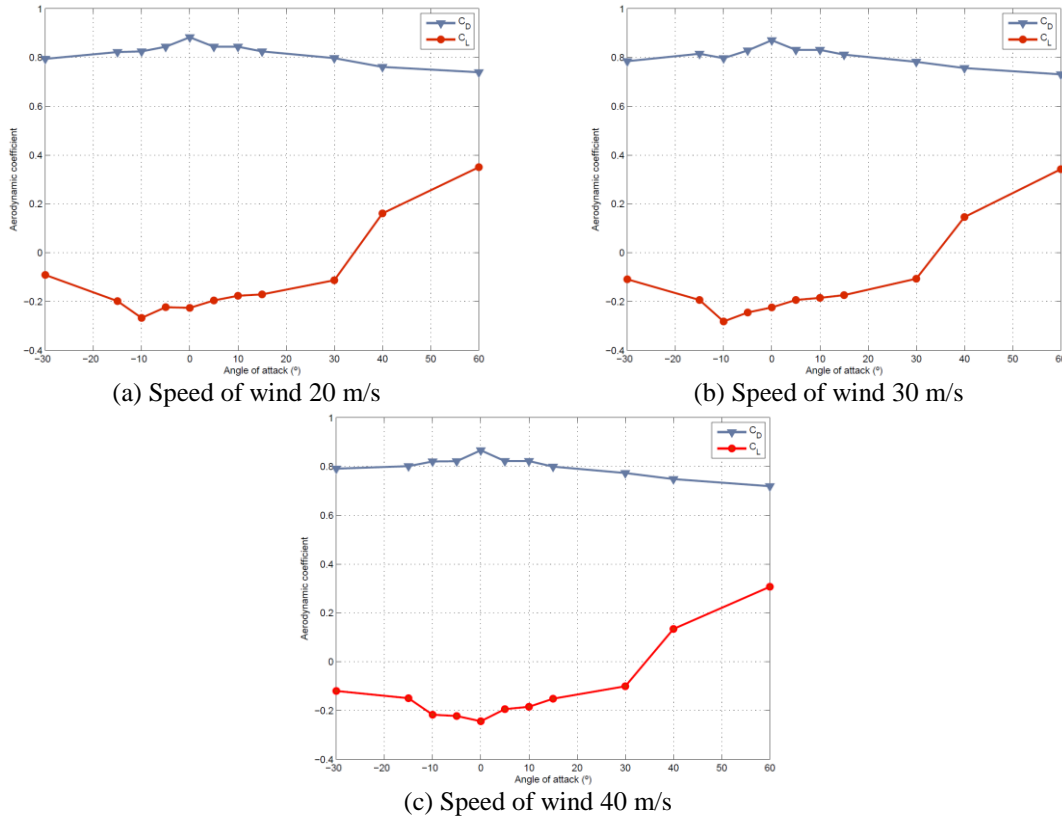


Fig. 6 Aerodynamic coefficients for AC-150 catenary cable

Finally, to ensure the validity of the models, some low speed ones have also been run. The most important result of those is the one obtained for an AC-150 cable, with an angle of attack of  $0^\circ$  and at a wind speed of 1 m/s. The  $C_D$  obtained in this case is 1.01, which being much higher than the others does not correspond to higher Reynolds number, as was expected. Nonetheless, it is quite close to the value of  $C_D=1.1$  given in Kiessling *et al.* (2001).

The negative lift coefficient that appears when the angle of attack is nearby 0 is due to the low pressure mentioned above. The tendency of the graph has been compared with those obtained within wind tunnel tests made by Yamaguchi (1990) and Gu *et al.* (2000). Both experiments tested the behavior of a cylinder under wind and rain loads, while the first one consists of water sprayed appropriately on the cable model to form a moving rivulet, the second one is obtained for an artificial rivulet stuck to the cable. Both referenced curves of  $C_L$  present similar shapes to the simulated ones, being  $C_L \approx 0$  for an angle of attack of around  $0^\circ$  and becoming positive as the flow comes from above.

Furthermore, as an additional result from this study, the den Hartog criterion has been applied to the AC-80 and AC-150 catenary cables at wind speed of 20, 30 and 40 m/s. Note in graphs from Figs. 7(a) and 7(b) that the cable could be aerodynamically unstable when the line is in the negative field, being stable otherwise. In particular for the cables studied and mostly in agreement

with Stickland and Scanlon (2001), angles of attack slightly negative could possibly become an unstable system, despite whether or not galloping would occur when this criterion is met ultimately depends upon the wire mass per unit length, the mechanical damping and the wind strength.

#### 4. FEM catenary analysis

Usually, rules and standards collect such kinds of wind loads by their catastrophic effects. Particularly, overhead catenary line design takes into account the extreme wind speed with a certain recurrence period. According to the European Standard EN 50119, see CENELEC (2009b), the wind speed that is used for the structural design of supports has a return period of 50 years, which means that from data taken over an average period of ten minutes this value is not exceeded in that return period. The Standard EN 50125-2 CENELEC (2002a) gathers values for 50 years of wind velocities.

Nevertheless, neither standards related to this topic nor technical publications takes into account the aerodynamic characteristics of the cables. It is implicitly assumed that the symmetry of the cables is not a true for the contact wires, as is described above, about all axes. To illustrate the relevance of an accurate cable characterization presented in this paper and to assess the effects of wind loads on railway overhead lines, the sensitivity of a basic criterion of design is analyzed. Among the classical design criteria of overhead catenary lines are those related to the stiffness distribution. The determination of this feature is widely known due to it involving computing the initial equilibrium of the cable structure. Thus, the procedures only based on the finite element method are inefficient at solving this complex problem, since they require expensive iterative processes to find the initial equilibrium or, namely in the railway topic, to determine the length of the droppers along the structure. Considering these limitations, prior to applying FEM for the stiffness distribution, the initial equilibrium is solved according to Such *et al.* (2009), a static calculation method of cable structures based on the analytical equation of the catenary.

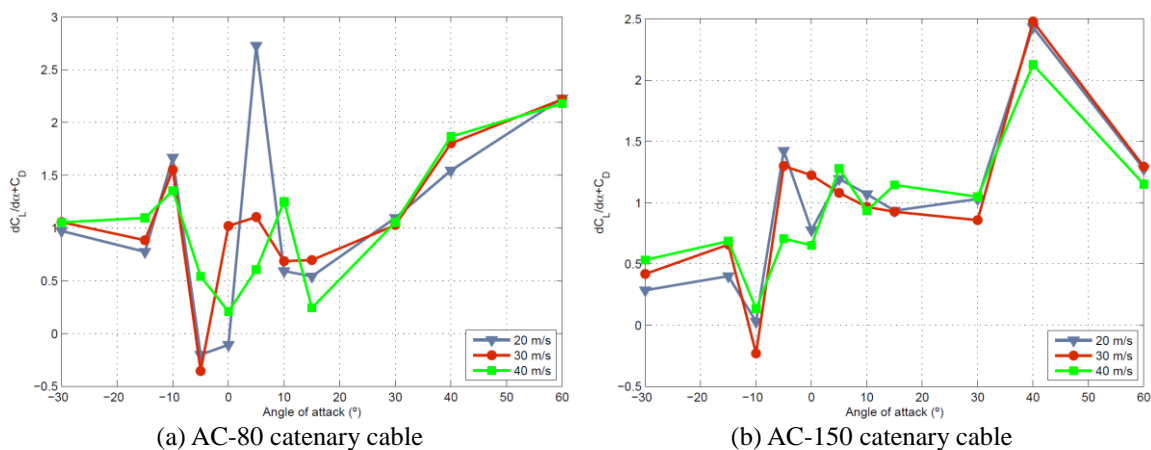


Fig. 7 Den Hartog criterion at different angles of attack

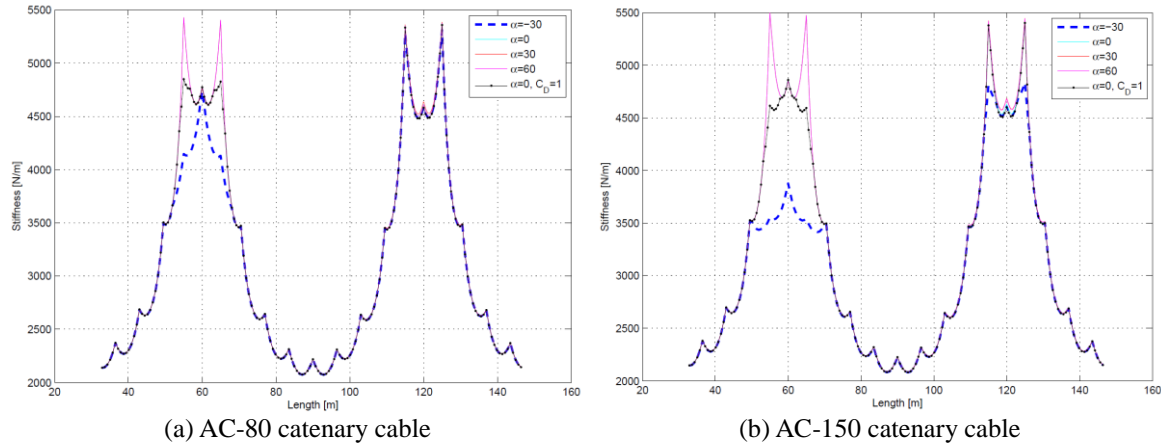


Fig. 8 Stiffness distribution at different angles of attack at wind speed of 20 m/s

Figs. 8(a) and 8(b) depict the stiffness distribution of a 60-meter-length-span, the benchmark model proposed in the standard EN 50318 by CENELEC (2002b), under different angles of attack of the wind load at 20 m/s. This parametric analysis based on different angles but uniquely one wind speed is based on Figs. 5(a)-5(c) and 6(a)-6(c), which show a strong dependence of the studied coefficients with the angles but much lower with the speed. Two different real cables for high speed trains are analyzed, AC-80 and AC-150, whose geometries were detailed in Table 1. The simulations have been carried out considering the drag and lift coefficients collected in Section 3.1 but compared with the most extended assumption considering  $C_D=1$ .

Both graphs evidence a significant influence of the angle of attack of the wind in the stiffness of the catenary near the steady arms of the span, located at 60 m and 120 m. Due to the zigzag of the contact wire along the railway path, the effect of lateral wind at the masts is highly dependent on whether this stagger is in favour or against the lateral wind. This effect is such that when it is against wind direction, first mast, stiffness decreases with the angle of attack. However, if zigzag is in favour of wind direction, according to the second mast, the stiffness of the system barely varies. Therefore it should be noted that important decreases of the stiffness in the closeness of steady arms may cause it to buckle. Then, the huge blow-off may cause serious consequences, such as loss of contact between catenary and pantograph and even its dewirement.

## 5. Conclusions

In this paper, a systematic study has been carried out to obtain the aerodynamic coefficients by means of CFD of a contact cable for overhead railway lines. Three wind speeds have shown to be in accordance with other studies to obtain the aerodynamic coefficients  $C_D$  and  $C_L$  for two types of contact cables and a wide enough range of angles of attack. Finally, this aerodynamic characterization has been applied to the static analysis of the stiffness distribution of a catenary span.

Due to the different lift coefficient obtained for different angles of attack, mainly from around  $30^\circ$  and independently to wind speed and cable, the first conclusion of this study is the relevance of the orography in the impact of the wind on the catenary. Cliffs and valleys could change the angle of attack or generate a vortex that affects the interaction with the wire. When the angle of attack is near  $0^\circ$ , a low pressure appears under the grooved cable that could benefit the contact between pantograph and wire. Nonetheless, the same low depression could boost the appearance of galloping phenomenon.

The second main conclusion of this work is focused on the effect of the lateral wind on the steady arms when the stiffness distribution is analyzed. Due to the stagger of the contact wire, the stiffness of the catenary in the closeness of a steady arm decreases with the angle of attack, which may cause it to buckle and lead to further risky consequences, such as loss of contact between catenary and pantograph and even dewirements. However, up to now, neither standards related to this topic nor technical publications have taken into account the lift force of the cables in overhead catenary lines.

## Acknowledgments

The authors gratefully acknowledge the financial support from the Spanish *Ministerio de Ciencia y Tecnología* under the project TRA2009-13912-C02-02 and *Ministerio de Ciencia e Innovación* under the project TRA2012-37940.

## References

- Alonso, G., Barrero, A., Meseguer, J. and Astiz, M.A. (2007a), "Ensayos aeroelásticos de un modelo de puente de arco sobre el río Tajo", *Ingeniería Aeronáutica y Astronáutica*, **383**, 37-43.
- Alonso, G. and Meseguer, J. (2006), "A parametric study of the galloping instability of two-dimensional triangular cross-section bodies", *J. Wind Eng. Ind. Aerod.*, **94**(4), 241-253.
- Alonso, G., Meseguer, J. and Perez-Grande, I. (2005), "Galloping instabilities of two-dimensional triangular cross-section bodies", *Exp. Fluids*, **38**(6), 789-795.
- Alonso, G., Meseguer, J. and Perez-Grande, I. (2007b), "Galloping stability of triangular cross-section bodies: a systematic approach", *J. Wind Eng. Ind. Aerod.*, **95**(9-11), 928-940.
- Barcala, M. and Meseguer, J. (2007), "An experimental study of the influence of parapets on the aerodynamic loads under cross wind on a two-dimensional model of a railway vehicle on a bridge", *J. Rail Rapid Transit*, **221**(4), 487-494.
- Bocciolone, M., Resa, F., Rocchi, D., Tosi, A. and Collina, A. (2006), "Pantograph aerodynamic effects on pantograph-catenary interaction", *Vehicle Syst. Dyn.*, **44**, 560-570.
- Brika, D. and Laneville, A. (1999), "The flow interaction between a stationary cylinder and a downstream flexible cylinder", *J. Fluid Struct.*, **13**(5), 579-606.
- CENELEC (2002a), "EN-50125-2. Railway applications. Environmental conditions for equipment Fixed electrical installations", *European Standard*.
- CENELEC (2002b), "EN-50318. Validation of simulation of the dynamic interaction between pantographs and overhead contact line", *European Standard*.
- CENELEC (2009a), "EN-15273:2. Railway applications - Gauges – Part 2: Rolling stock gauge", *European Standard*.
- CENELEC (2009b), "EN-50119. Railway applications - Fixed installations - Electric traction overhead

- contact lines”, *European Standard*.
- Collina, A., Fachinetti, A. and Resta, F. (2007), “A feasibility study of an aerodynamic control for high speed pantograph”, *Proceedings of the International Conference on Advanced Intelligent Mechatronics*.
- European Railway Agency (2009), “Trans-European conventional rail system. Technical Specification of Interoperability”.
- Flamand, G. and Leclair, J. (2005), “Galloping of tramway catenary”, *Proceedings of the 4th European & African Conference of Wind Engineering*.
- Gu, M., Xu, Y., Liu, C. and Xiang, H. (2000), “Wind tunnel study of response characteristics of cables with artificial rivulet”, *Proceedings of the International Conference on Advances in Structural Dynamics*.
- Gurung, C., Yamaguchi, H. and Yukino, T. (2003), “Identification and characterization of galloping of Tsuruga test line based on multichannel modal analysis of field data”, *J. Wind Eng. Ind. Aerod.*, **91**(7), 903-924.
- Holmes, J.D (2015), *Wind loading of structures*, 3rd Ed., CRC Press, Boca Raton, Florida, USA.
- Hover, F. and Triantafyllou, M. (2001), “Galloping response of a cylinder with upstream wake interference”, *J. Fluid Struct.*, **15**(3-4), 503-512.
- Imai, T., Fujii, T., Tanemoto, K., Shimamura, T., Maeda, T., Ishida, H. and Hibino, Y. (2002), “New train regulation method based on wind direction and velocity of natural wind against strong winds”, *J. Wind Eng. Ind. Aerod.*, **90**(12-15), 1601-1610.
- Johnson, T. (1996), “Strong wind effects on railway operations”, *J. Wind Eng. Ind. Aerod.*, **60**, 251-266.
- Kiessling, F., Puschmann, R. and Schmeider, A. (2001), “Contact Lines for Electric Railways”, Munich Erlangen.
- Kwon, H., Park, Y., Lee, D. and Kim, M. (2001), “Wind tunnel experiments on Korean high-speed trains using various ground simulation techniques”, *J. Wind Eng. Ind. Aerod.*, **89**(13), 1179-1195.
- Liu, Z., Song, Y., Wang, Y., Wang, H. and Gao, S. (2014), “The catenary vibration response of high-speed electrified railway considering horizontal wind”, *Proceedings of the 2013 International Conference on Electrical and Information Technologies for Rail Transportation*.
- Meseguer, J., Sanz, A., Perales, J. and Pindado, S. (2001), *Aerodinámica civil. Cargas de viento en las edificaciones*, McGraw-Hill, New York.
- Paidoussis, M., Price, S. and Langre, E. (2011), *Fluid-Structure Interactions: Cross-Flow-Induced Instabilities*, Cambridge University Press, Cambridge, U.K.
- Stickland, M., Scalon, T., Craighead, I. and Fernandez, J. (2003), “An investigation into mechanical damping characteristics of catenary contact wires and their effect on aerodynamic galloping instability”, *Rail Rapid Transit*, **217**(2), 63-71.
- Stickland, M., Scalon, T. and Oldroyd, A. (2000), “An investigation into the attenuation of wind speed by the use of windbreaks in the vicinity of overhead wires”, *Rail Rapid Transit*, **214**(3), 173-182.
- Stickland, M. and Scalon, T. (2001), “An investigation into the aerodynamic characteristics of catenary contact wires in a cross-wind”, *Rail Rapid Transit*, **215**(4), 311-318.
- Such, M., Jimenez-Octavio, J., Carnicero, A. and Lopez-Garcia, O. (2009), “An approach based on the catenary equation to deal with static analysis of three dimensional cable structures”, *Eng. Struct.*, **31**(9), 2162-2170.
- Suzuki, M., Tanemoto, K. and Maeda, T. (2003), “Aerodynamic characteristics of train/vehicles under cross winds”, *J. Wind Eng. Ind. Aerod.*, **91**(1-2), 209-218.
- Yamaguchi, H. (1990), “Analytical study on growth mechanism of rain vibration of cables”, *J. Wind Eng. Ind. Aerod.*, **33**(1-2), 73-80.
- Zdero, R. and Turan, F. (1995), “Toward understanding galloping: nearwake study of oscillation smooth and stranded circular cylinders in forced motion”, *Exp. Therm. Fluid Sci.*, **10**(1), 28-43.
- Zheng, S. (2009), “Research on the wind load parameters and the wind fences behaviour for wind fences of railway bridge”, *Proceedings of the 7th Asia-Pacific Conference on Wind Engineering*.